Synthesis and characterization of aldamine condensed Schiff bases and their iron salts

Chao Meng[1] (ORCID ID: 0000-0001-6603-2273)**, Zheng Gu**[1), 2), 4), 5), *] (0000-0001-9521-2863)**, Jianfa Wang**[1] (0000-0002-1242-3794)**, Jinyong Sui**[1] (0000-0002-4232-3540)**, Shaokai Hu**[1] (0000-0002-2049-3135)**, Susu Zhang**[1] (0000-0003-3620-0816)**, Xiaoyi Zhang**[1] (0000-0003-4047-5046)**, Peiyao Li**[3] (0000-0002-4713-1599)**, Wenjin Liu**[3] (0000-0001-5563-1801)**, Yifan Hu**[3] (0000-0002-3608-5419)

Abstract: Two types of long-chain conjugated Schiff bases and their iron salts were obtained by the coordination polycondensation of *p*-phenylenediamine with glyoxal or terephthalaldehyde. Elemental analysis and infrared spectroscopy (FTIR) were used to evaluate the chemical structure of the obtained poly(Schiff bases) and their salts. Thermal stability (TGA) and electrical conductivity were also investigated.

Keywords: glyoxal, terephthalaldehyde, Schiff bases, electrical conductivity.

Synteza i charakterystyka skondensowanych zasad Schiffa i ich soli żelaza z aldaminą

Streszczenie: W wyniku koordynacyjnej polikondensacji *p*-fenylenodiaminy z glioksalem lub aldehydem tereftalowym otrzymano dwa rodzaje długołańcuchowych sprzężonych zasad Schiffa oraz ich sole żelazowe. Do oceny struktury chemicznej otrzymanych zasad Schiffa i ich soli stosowano analizę elementarną i spektroskopię w podczerwieni (FTIR). Zbadano również stabilność termiczną (TGA) i przewodnictwo elektryczne.

Słowa kluczowe: glioksal, aldehyd tereftalowy, zasady Schiffa, przewodność elektryczna.

Electromagnetic radiation is a wave-like form of energy emitted or absorbed by charged particles. Electromagnetic radiation has been present in the surrounding environment for as long as people can remember. Although its main source is the sun, all animals, plants, and humans also generate weak electromagnetic fields. However, in the era of electricity, the so-called artificial electromagnetic radiation produced by various electrical appliances, mobile phones, satellites, radio, and television towers, began to appear, and gather around. This radiation is called electromagnetic smog or electromagnetic interference (EMI).We have been unknowingly surrounded by electromagnetic smog (EMI). How to avoid the damage from electromagnetic radiation has become a hot research topic [1]. At the same time, related scholars were also conducting various studies. The most common EMI shielding materials are metals due to their high electrical conductivity. However, their high density, low flexibility, susceptibility to corrosion, and heavy processing or handling limit the use of metals and metal composites in modern devices. To overcome the limitations of metal-based electromagnetic shielding materials, much attention has been paid to polymeric and composite materials due to their advantages such as easy processing, easy bending, low specific gravity, resistance to chemical corrosion, and adjustable structural and mechanical properties.

In the field of fifth generation (5G) communications, people have high demands on flexible, lightweight and high-performance EMI shielding materials. As a wave absorbing material, Schiff bases have many advantages, such as adjustable electromagnetic content, light specific gravity, high stability and good compatibility with resins. They have developed rapidly in recent years. However, the preparation of absorbing materials is complicated. On this basis, according to the Hugan-Rubens approximation theory, high conductivity Schiff bases have some infrared stealth properties [2].

[1] College of Chemistry and Chemical Engineering, Qingdao University, Ningxia Road, Qingdao, Shandong 266071, China.

[2] Weihai Innovation Institute, Qingdao University, Ningxia Road, Qingdao, Shandong 264200, China.

[3] College of materials science and Engineering, Qingdao University, Ningxia Road, Qingdao, Shandong 266071, China.

[4] Weifang Key Laboratory of Environmentally Friendly Macromolecular Flame Retardant Materials, Weifang 262715, China.

[5] Shandong Engineering Laboratory of Environmentally Friendly Macromolecular Flame Retardant Materials, Weifang 262715, China.

*) Author for correspondence: guzheng596@163.com

According to the structural design, detailed studies were carried out, and a rational explanation of the absorption mechanism of the absorbing material was given. Theoretically, this work improves methods for studying the synthesis and absorption mechanisms of long-chain conjugates of poly(Schiff bases) and their metal salts. In practice, conducting studies of the Schiff bases conductivity has a huge impact on the future direction of research [3]. Inherently conductive polymers with delocalized conjugated electronic structures have remarkable electronic properties such as low ionization potential, high electron affinity and electrical conductivity, which can be significantly improved by chemical synthesis or compound doping. Commonly used polymers are typical electrical insulators. Therefore, they cannot provide a shielding effect. However, the introduction of appropriate polymers can give polymer composites unique electromagnetic properties. The use of appropriate composite fillers or filler combinations can not only adjust the physical and mechanical properties of polymer composites, but also adjust the dielectric constant, permeability, thermal conductivity and electrical conductivity or thickness to achieve better EMI performance. Both p-phenylenediamine and terephthalaldehyde have large π conjugate systems.

Glyoxal is a simple active monomer containing carbonyl groups, which are continually active, and react easily. Besides, glyoxal is cheap and easy to obtain. The introduction of a large π bond of the benzene ring increases the conjugate system of the Schiff base material, and the number of π electrons increases to form an electron-rich system. The amino group is easy to coordinate with metal ions, which can effectively improve the coordination conductivity [4].

Absorption principle of long-chain conjugated Schiff bases

Figure 1 shows the molecular structure of long-chain conjugated Schiff bases. The principle of material absorption is to delay absorption, transfer loss, and convert electric energy into thermal energy or other forms. According to the absorption characteristics, the material absorption radar can be divided into two types: electrical loss and self-loss. It is mainly the real part of the magnetic material, which reduces the wavelength propagation transparency, and the virtual part of the magnetic substance, which reduces the electrons energy; in the absorption of lossy wave materials. This is mainly achieved by electrodes and conduction, while the material is a two-dimensional plane with many long-chain conjugated large π bonds connected to multi-component chain units on the main chain. By radar waves, coupled with long chain Schiff base, it transfers charges through the conjugation of single and double bonds. Electrons can move along the long chain, and its atoms are rearranged, thus changing the electromagnetic parameters to absorb radar waves [6].
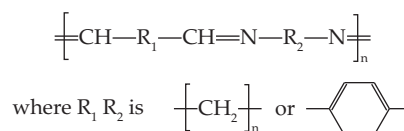

Fig. 1. Structural formula of long chain conjugated Schiff bases

Assumptions design

Schiff bases and their salts can easily coordinate with metal ions to form complexes due to their own C=N bonds. Magnetic metal particles and their alloys and other traditional absorbing materials have the disadvantages of high density, poor environmental stability, poor absorption of electromagnetic waves and narrow absorption frequency bands, which do not meet the comprehensive goals of "thin, light, wide, and strong", which limits their application [7]. Long-chain conjugated poly(Schiff bases) have good wave-absorbing properties and high electrical conductivity, and are appreciated by scientists for their adjustable electrical and magnetic doping, light specific gravity, high stability, and good compatibility. Composite materials obtained by synthesizing their salts or adding dopants have significantly improved electrical conductivity and wave-absorbing properties [8]. According to relevant research reports, Schiff bases and their salts have good microwave absorption properties in the semiconductor range.

Therefore, in recent years Schiff bases and their salts have become the subject of research by many scientists. The special electronic structure of the iron-metal elements (the outermost layer is $3d^{6}4s^{2}$) and electromagnetic properties and special effects of nanomaterials have also attracted attention in the field of electromagnetics.

Although there are many reports of small molecule Schiff bases and their salts in the field of wave absorption, however, there are only few studies on macromolecular conjugated Schiff bases [9]. Therefore, this paper initially synthesized two kinds of long-chain conjugated Schiff bases using glyoxal, terephthalaldehyde, and p-phenylenediamine as raw materials, and then synthesized the corresponding iron salts of Schiff bases by reacting with transition metal iron salts, respectively]. The synthesized samples were characterized and tested by elemental analyzer, FTIR, four-probe conductivity meter and TG. It was reported that the structure of Schiff alkali metal salts does affect the electrical conductivity and wave-absorbing properties of the material, which lays the foundation for further research. The absorption properties of Schiff bases can be improved by adjusting the electrical conductivity by coordinating metal ions, designing the matrix and introducing a chiral helical structure [8–12].

Thus, in this paper, two types of long-chain conjugated Schiff bases and their salts were obtained as a result of coordination polycondensation of p-phenylenediamine with glyoxal or terephthaldehyde. FeCl$_3$ was used for coordination to obtain a properly conjugated Schiff base [5]. Elemental analysis and infrared spectroscopy (FTIR)

were used to evaluate the chemical structure of the obtained Schiff bases and their salts. Thermal stability (TGA) and electrical conductivity were also investigated.

EXPERIMENTAL PART

Materials

P-phenylenediamine ($C_6H_8N_2$), anhydrous ferric chloride ($FeCl_3$), anhydrous ethanol (C_2H_5OH), glyoxal ($C_2H_2O_2$), terephthalaldehyde ($C_8H_6O_2$), and acetic acid (CH_3COOH) were purchased from Sinopharm Group Chemical Co., Ltd, China.

Methods

The chemical structure of Schiff bases and their salts was evaluated using elemental analyzer (Thermo Fisher scientific). The C, H, O, N, and S were determined [14]. The chemical structure was also analyzed by Fourier infrared (FTIR) spectroscopy (PerkinElmer Instruments Ltd, Switzerland). The spectra were recorded using at least 32 scans with 2 cm^{-1} resolution, in the spectral range 4000−500 cm^{-1}, using KBr pellets technique. Electrical conductivity was measured using four-probe conductivity meter (Guangzhou Four Probe Technology Co. Ltd, China). Samples with a diameter of 30 mm and a thickness of < 2 mm were obtained by pressing on gold thin-layer electrodes (pressure 10 MPa, press time 2 min) and vacuum-evaporation. The test voltage was 10-100 V [15]. Thermal stability was determined by thermogravimetric analysis (TGA) using TGA/STA-500 thermogravimetric analyzer (Thermo Fisher Scientific,) in nitrogen atmosphere at heating rate of 10°C/min, from 25 to 1400°C [16].

Synthesis of terephthalaldehyde condensed *p*-phenylenediamine long –chain conjugated poly(Schiff base) L1 and its iron salt C1

Poly(Schiff base) L1 and its iron salt C1 were synthesized according to the procedure reported elsewhere [17]. Briefly, p-benzaldehyde (0.12 mol) was dissolved in 180 mL of absolute ethanol, and then the solution was slowly dropped under the protection of N_2 to the solution of *p*-phenylenediamine (0.12 mol) in 240 mL of anhydrous ethanol. The resulting mixture was heated at 75°C under reflux for 8 hours and then sonicated for 15 minutes. The samples were filtered under reduced pressure and washed with distilled water and absolute ethanol,
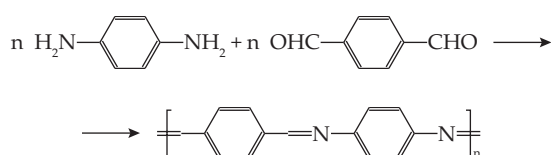
respectively. The process was repeated 3−4 times. The product was dried in a vacuum at temperature 50°C for 12 h. A golden yellow powder with a melting point of 320°C (yield 75%) was obtained. The synthesis route of poly(Schiff base) condensed from *p*-phenylenediamine and terephthalaldehyde is shown in Figure 2.

P-phenylenediamine (0.12 mol) was fully dissolved in 240 mL of anhydrous ethanol and transferred it into a 500 mL three-necked flask. A small amount of glacial acetic acid was added as a catalyst. The mixture was heated to 72°C and stirred until complete dissolution. Afterwards, the solution of *p*-benzaldehyde (0.12 mol) in 180 mL of absolute ethanol was slowly dropped into the reaction mixture. Then anhydrous $FeCl_3$ (0.12 mol) dissolved in 180 ml of anhydrous ethanol was also slowly dropped. The color of the solution gradually changed from orange-red to deep-brown. After dripping was complete, the reaction mixture was heated to 75°C and the process continued under nitrogen protection for 8 hours. The washing, filtering and drying procedure was the same as for poly(Schiff's base) L1. The reaction yield was 64%. The synthesis of poly(Schiff base) iron salt C1 is shown in Figure 3.
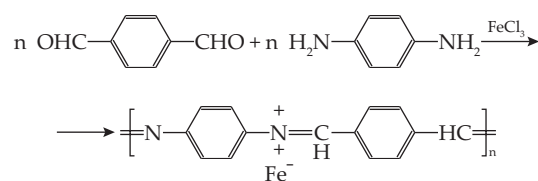

Fig. 3. Synthesis o of *p*-phenylenediamine poly(Schiff base) iron slat (C1) condensed from terephthalaldehyde

Synthesis of glyoxal condensed *p*-phenylenediamine long chain conjugated poly(Schiff base) L2 and its iron salt C2

Poly(Schiff base) L2 and its iron salt C2 were synthesized according to the procedure reported elsewhere [17]. Briefly, glyoxal (0.12 mol) was fully dissolved in anhydrous ethanol (120 mL) and added to the solution of *p*-phenylenediamine (0.12 mol) in 240 mL of anhydrous ethanol. The process was carried out at 75°C for 8 h in the nitrogen atmosphere. The color of the solution changed from yellow to reddish-brown. After cooling to room temperature, the sample was filtered, washed and dried as poly(Schiff's base) L1 to give an orange-red powder. The reaction yield was 84%, melting point 340°C.
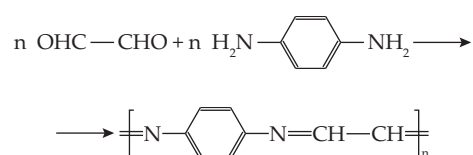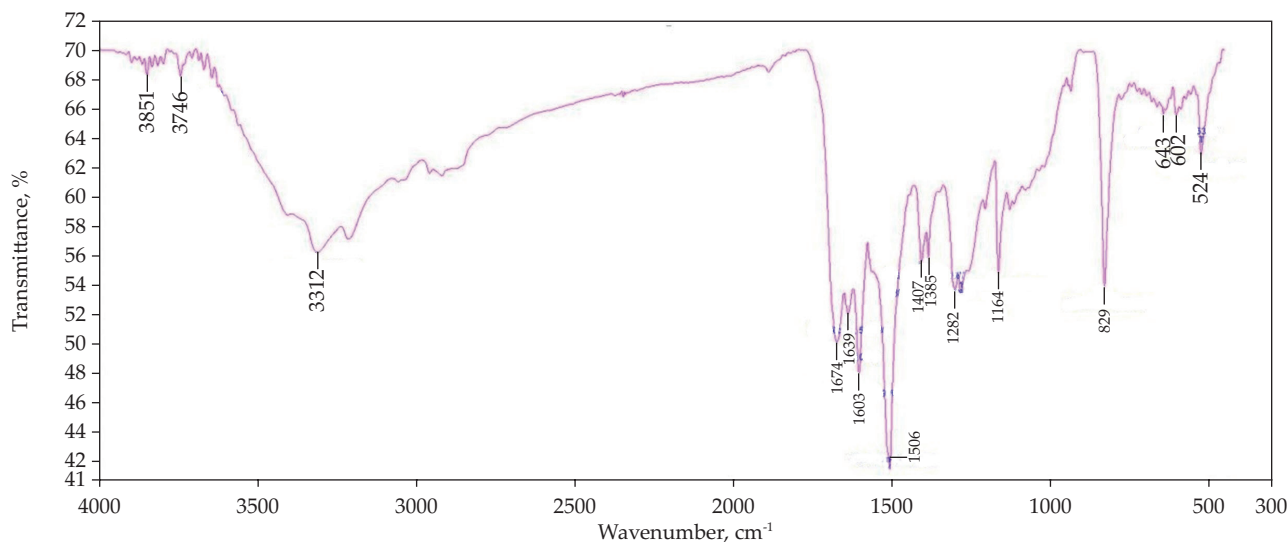

Fig. 2. Synthesis of terephthalaldehyde condensed *p*-phenylenediamine poly(Schiff base) L1

Fig. 4. Synthesis of glyoxal condensed *p*-phenylenediamine poly(Schiff base) L2

T a b l e 1. Elemental analysis of poly(Schiff bases)

Poly(Schiff base)	Molecular formula	Measured (calculated)		
		C, %	H, %	N, %
L1	$(C_{14}H_{10}N_2)_n$	80.82 (81.49)	4.85 (4.86)	13.45 (13.65)
L2	$(C_8H_6N_2)_n$	73.24 (73.89)	4.47 (4.61)	21.31(21.50)

Fig. 5. FTIR spectrum of poly(Schiff base) L1

Glyoxal (0.12 mol) was fully dissolved in anhydrous ethanol (120 mL) and added to the solution of *p*-phenylenediamine (0.12 mol) in 240 mL of anhydrous ethanol. During the process, 0.12 mol of anhydrous $FeCl_3$ dissolved in 180 mL of anhydrous ethanol was slowly added dropwise to the reaction mixture. The process was carried out at 75°C for 8 h in the nitrogen atmosphere. The color of the solution changed from orange-red to black. After cooling to room temperature, the sample was filtered, washed and dried as poly(Schiff's base) L1. The reaction yield was 73%. The synthesis of poly(Schiff base) iron salt C2 is shown in Figure 4.

RESULTS AND DISCUSSION

Elemental analysis

Elemental analysis was used to determine the content of C, H, N, and O elements in the obtained poly(Schiff bases), and the results are summarized in Table 1. No oxygen was found in the obtained products, which proves the complete conversion of terephthalaldehyde. It should be noted that the determined content of elements is very close to the theoretical values.

FTIR analysis

FTIR was used to characterize the chemical structure of obtained poly(Schiff bases) (L1, L2) and their iron salts (C1, C2). FTIR spectrum of poly(Schiff bases) L1 (Fig. 5) shows the following peaks: at 3313 cm^{-1} (primary amine stretching vibration), 1603 cm^{-1} (C=N stretching vibra-

tion), 1507 cm^{-1} (benzene ring stretching vibration), and 975−800 cm^{-1} (1,4-substituted benzene ring) [10], confirming the structure of the product synthesized according to the reaction presented in Fig. 2.

FTIR spectra of poly(Schiff base) iron salt C1 is presented in Figure 6. The peak at 3442 cm^{-1} is associated to the primary amine stretching vibration. The band at 1612 cm^{-1} is related to C=N vibration, the bands at 1488 cm^{-1} and 1413 cm^{-1} with benzene (stretching vibration of ring skeleton 1,4 substitution), and the band at 567 cm^{-1} is assigned to N-Fe^{3+} [8].

Comparing the L1 and C1 infrared data, it can be seen that the aromatic peaks of the amine and C=N stretching vibrations are shifted towards lower wavenumbers. This indicates that *p*-benzaldehyde is condensed with *p*-phenylenediamine Schiff base iron salt; after the formation of the salt, the electrons of the lone pair of the Schiff base nitrogen atom are attracted to the π orbitals of the iron ion, forming coordination bonds. The density of the electron cloud on the aromatic group is high and the degree of coupling is strong, resulting in a shift in the FTIR spectrum bands.

FTIR spectrum of poly(Schiff base) L2 is shown in Figure 7. The peak about 3432 cm^{-1} is attributed to primary amine stretching vibration, 1638 cm^{-1} to C=N stretching vibration, 1508 cm^{-1} and 1407 cm^{-1} to aromatic ring skeleton stretching vibration, 1048 cm^{-1} to C-N bond connected by the benzene ring skeleton, and 676 cm^{-1} to the 1,4-position substitution stretching vibration of the benzene ring skeleton [13].

FTIR spectrum of poly(Schiff base) iron salt C2 is shown in Figure 8. The peak at 3199 cm^{-1} is associated
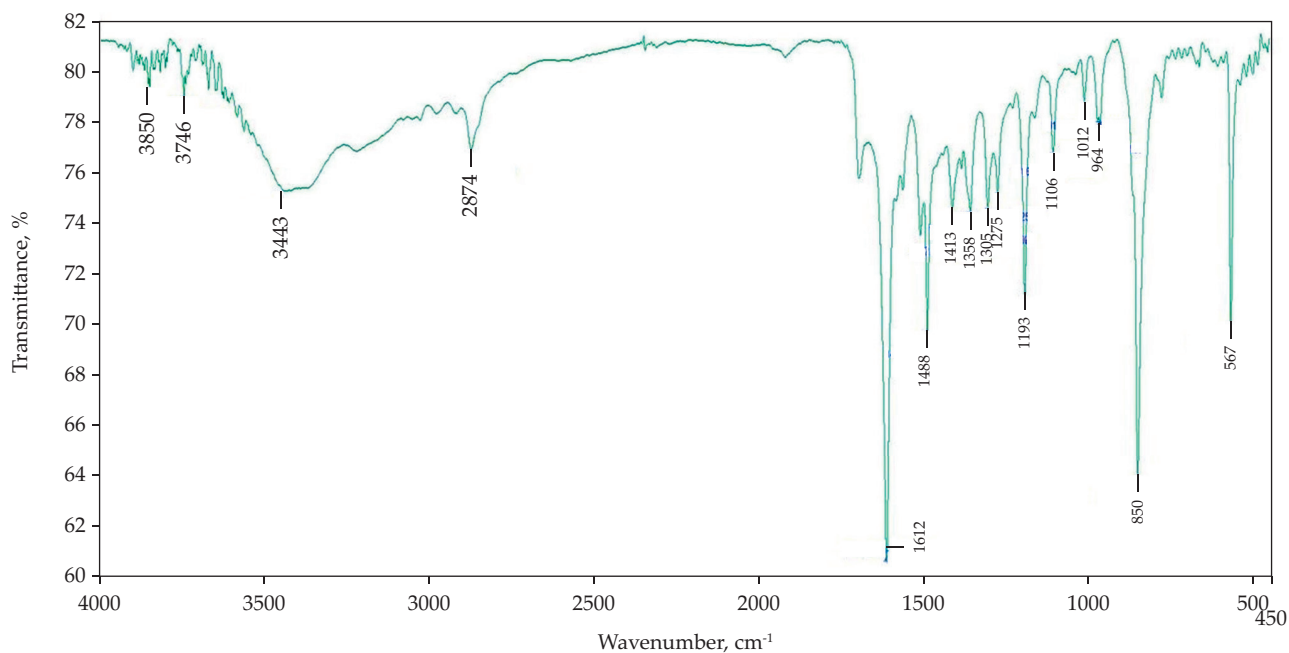
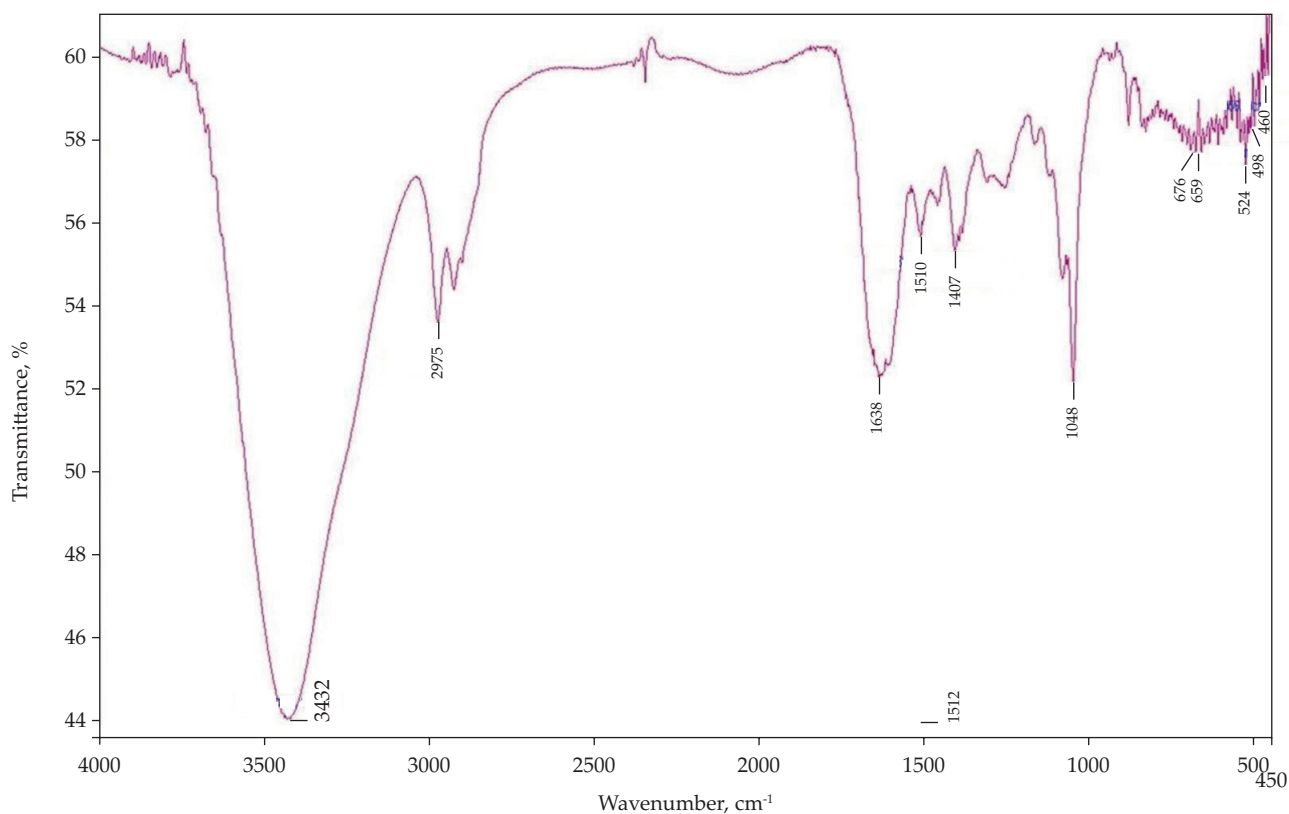Fig. 6. FTIR spectrum of poly(Schiff base) C1

Fig. 7. FTIR spectrum of poly(Schiff base) L2

with primary amine stretching vibrations, 1626 cm^{-1} with C=N bond stretching vibrations, 1512 cm^{-1}, 1403 cm^{-1} and 1312 cm^{-1} with aromatic ring C=C bond stretching vibrations, 832 cm^{-1} for the stretching vibration of the 1,4-substituted benzene ring, and 551 cm^{-1} for the vibrations of the N-Fe^{3+} coordination bond.

Comparing the L2 and C2 FTIR spectra, it can be seen that the aromatic peaks of the amine and C=N stretching vibrations are slightly shifted towards lower values. This indicates that *p*-benzaldehyde is condensed with *p*-phenylenediamine Schiff base iron salt [8, 13].

Conductive properties of poly(Schiff bases) and iron salts

The intrinsic conductivity of all synthesized poly(Schiff bases) and iron salts is summarized in Table 2. L1 showed higher conductivity than L2. The salts had a much higher
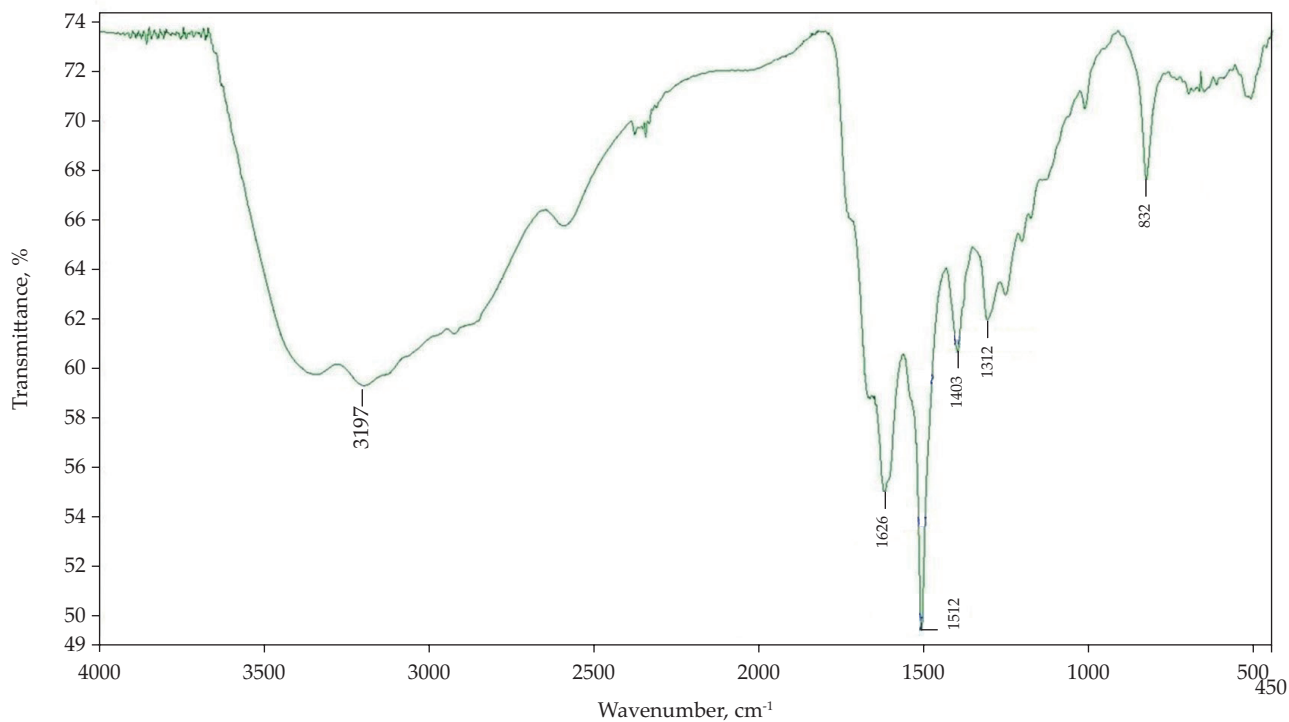
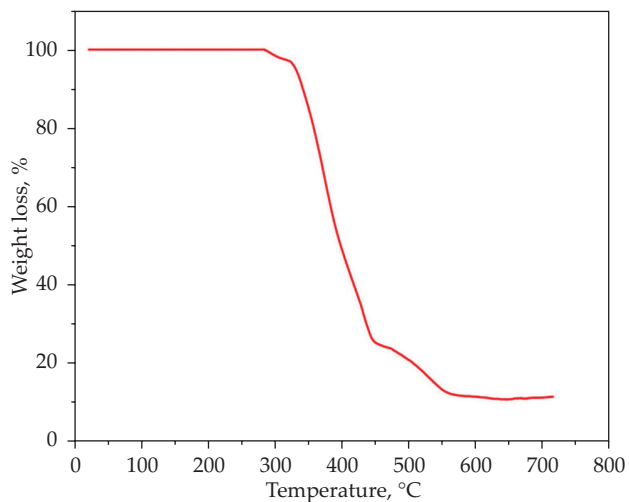**Fig. 8. FTIR spectrum of poly(Schiff base) iron salt C2**
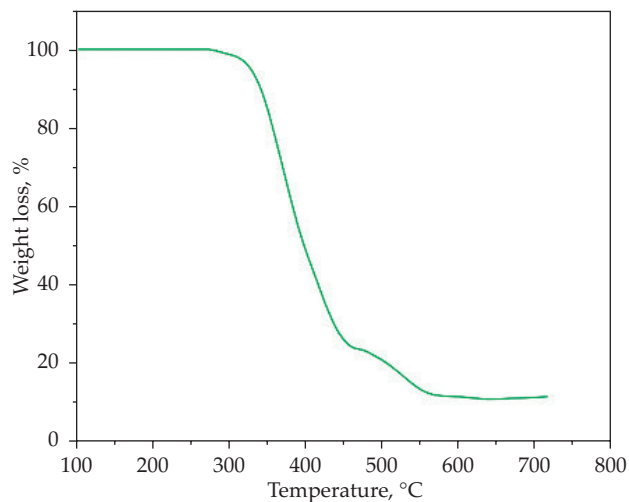

Fig. 9. TGA curve of poly(Schiff base) L1

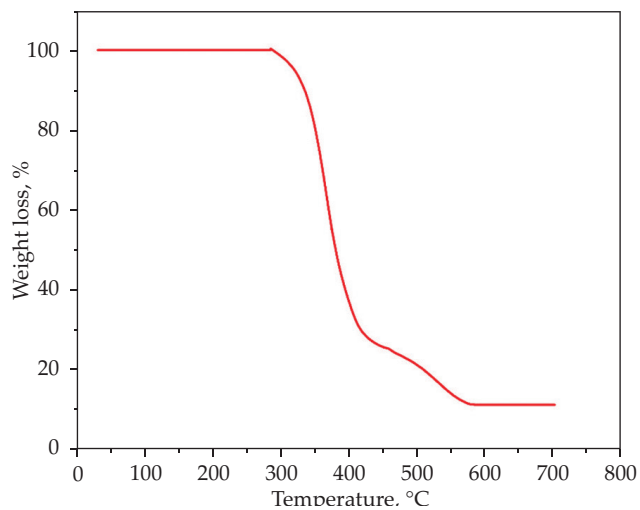**Fig. 10. TG curve of poly(Schiff base) iron salt C1**
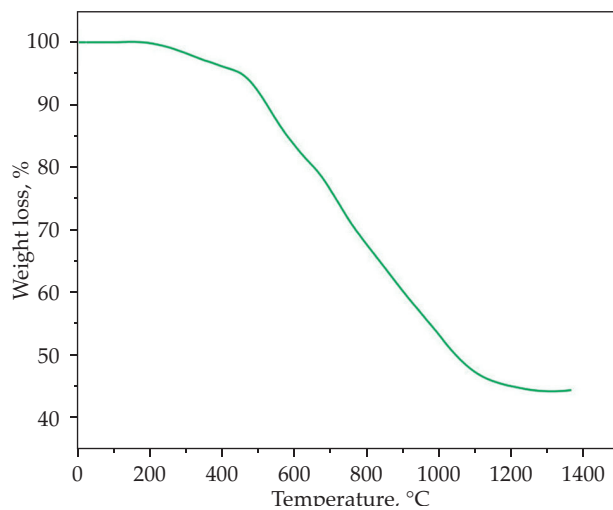

Fig. 11. TGA curve of poly(Schiff base) L2

Fig. 12. TGA curve of poly(Schiff base) iron salt C2

T a b l e 2. Conductivity of poly(Schiff bases) and their iron salts

Poly(Schiff base)	Conductivity, S/cm
L1	5.0×10^{-8}
L2	2.6×10^{-8}
C1	4.3×10^{-7}
C2	5.6×10^{-6}

conductivity than the corresponding bases, with the conductivity of C1 being much less than that of C2. This can be explained by the loss of electrons due to the coordination bond between the base nitrogen atom and the iron, and the presence of conjugated single and double bonds, thus improving the conductivity.

TGA analysis

The thermal degradation and stability of poly(Schiff bases) and their iron salts were determined from the TGA curves that were plotted as the percentage sample weight loss against temperature, as presented in Figs. 9–12. A two-stage degradation process can be observed for L1, L2 and C1 and a one-stage degradation process for C2. The first stage occurred below 300°C. The decomposition trend is plateau, indicating that poly(Schiff bases) and their iron salts have good stability up to 300°C. In the temperature range of 300–450°C, there is a rapid decomposition of poly(Schiff's bases). The skeleton of poly(Schiff base) is decomposed during this period, and the weight loss rate stabilizes after 555°C, with a residue of about 10%. It can be explained by the carbon deposition caused by the inorganic salt of Fe^{3+} and the carbon deposition effect.

It can be concluded that L1, L2 and C1 are stable up to 300°C. However, C2 decomposes already above 200°C. The rapid decomposition of this salt occurs in the temperature range of 200–1000 with a significantly bigger residue at 1400°C (45%). This is due to the accumulation of carbon deposits caused by inorganic Fe^{3+} salts and the carbon deposition effect.

CONCLUSIONS

Elemental analysis and FTIR confirmed the structure for poly(Schiff bases) and their iron salts, as evidenced by the presence of the -C=N- and Fe-N coordination bonds, respectively. L1, L2 and C1 are stable up to 300°C. In contrast, C2 decomposes already above 200°C with a significantly bigger residue (45%). In addition, poly(Schiff base)

salts show much better electrical conductivity than the corresponding poly(Schiff bases), increasing the conjugated effect, which may also result in a bigger magnetic effect.

REFERENCES

[1] Guo Y.J.: *Engineering Technology*, **2017**.
[2] Hu Y.X., Zhang H.Y., Xu G.Y. *et al.*: *Material Development and Application* **2016**, *31(01)*, 55.
[3] Hu Y.X.: *Nanjing University of Aeronautics and Astronautics* **2016**.
[4] Liu H.L.: *Nanchang Aviation University* **2012**.
[5] Liu H.L., Liu C.B., Chen Y. *et al.*: *Material Development and Application* **2012**, *26(13)*, 89.
[6] Dong Y., Yang C.B., Zhang D. *et al.*: *Application of Functional Coatings on Radar Equipment Environmental Engineering*, **2013**, *10(02)*, 48.
[7] Feyzi S.T., Parham T., Hande U. *et al.*: *Journal of Molecular Structure* **2021**, *1231*, 28.
https://doi.org/10.1016/j.molstruc.2020.129666
[8] Rao Arsalan K., Sajjad A., Luciana R. *et al.*: *Frontiers of Structural and Civil Engineering* **2016**, *10(2)*, 9.
https://doi.org/10.1007/s11709-016-0330-5
[9] Chen Y.J., Li Y.: *Composites Part B: Engineering* **2015**, *70*, 1.
https://doi.org/10.1016/j.compositesb.2014.11.006
[10] Ye X.Z., Hu J., Li B. *et al.*: *Chemical Engineering Journal* **2019**, *361*,11.
https://doi.org/10.1016/j.cej.2018.12.047
[11] Huang Y.W., Wang Y.J., Wei S.C. *et al.*: *International Journal of Modern Physics B* **2019**, *33(13)*,1.
https://doi.org/10.1142/S0217979219400551
[12] Rao A.K., Sajjad A., Luciana R. *et al.*: *Heliyon* **2019**, *5*, 17.
https://doi.org/10.1016/j.heliyon.2019.e01789
[13] Zhang M., Cao W.Q., Yuan J. *et al.*: *Advanced Optical Materials* **2019**, *7*, 34.
https://doi.org/10.1002/adom.201900689
[14] Reda M.E., Abdel S.: *Polymer Composites* **2012**, *33*, 532.
https://doi.org/10.1002/pc.22186
[15] Wu Y.M., Qi S.H., Wang D.H. *et al.*: *Chemical Industry and Engineering* **2008**, *25*, 82.
[16] Ding C.X., Fan C.B., Zhang L.H. *et al.*: *Material Development and Application* **2006**, *35(04)*, 4.
[17] Wang J., Gu Z., Zhang S. *et al.*: *Polimery* **2022**, *67*, 20.
https://doi.org/10.14314/polimery.2022.1.3